

Article

Probing Differential Metabolome Responses among Wheat Genotypes to Heat Stress Using Fourier Transform Infrared-Based Chemical Fingerprinting

Salma O. M. Osman^{1,2}, Abu Sefyan I. Saad², Shota Tadano¹, Yoshiki Takeda³, Yuji Yamasaki⁴,
Izzat S. A. Tahir² , Hisashi Tsujimoto⁴  and Kinya Akashi^{1,3,4,*} 

- ¹ United Graduate School of Agricultural Sciences, Tottori University, 4-101 Koyama-Chou-Minami, Tottori 680-0945, Japan; d19a3112u@edu.tottori-u.ac.jp (S.O.M.O.); d18a3002z@edu.tottori-u.ac.jp (S.T.)
² Agricultural Research Corporation, Wad Medani P.O. Box 126, Sudan; abusefianisaad@gmail.com (A.S.I.S.); izzatahir1@gmail.com (I.S.A.T.)
³ Faculty of Agriculture, Tottori University, 4-101 Koyama-Chou-Minami, Tottori 680-0945, Japan; m22j7026z@edu.tottori-u.ac.jp
⁴ Arid Land Research Center, Tottori University, 1390 Hamasaka, Tottori 680-0001, Japan; yujiyamas@tottori-u.ac.jp (Y.Y.); tsujim@tottori-u.ac.jp (H.T.)
* Correspondence: akashi.kinya@tottori-u.ac.jp; Tel./Fax: +81-857-31-5352

Abstract: Heat stress is one of the major environmental constraints for wheat production; thus, a comprehensive understanding of the metabolomic responses of wheat is required for breeding heat-tolerant varieties. In this study, the metabolome responses of heat-tolerant genotypes Imam and Norin 61, and susceptible genotype Chinese Spring were comparatively analyzed using Fourier transform infrared (FTIR) spectroscopy in combination with chemometric data mining techniques. Principal component analysis of the FTIR data suggested a spectral feature partially overlapping between the three genotypes. FTIR spectral biomarker assay showed similar heat responses between the genotypes for markers Fm482 and Fm1502, whereas genotype-dependent variations were observed for other markers. The markers Fm1251 and Fm1729 showed contrasting behaviors between heat-tolerant and susceptible genotypes, suggesting that these markers may potentially serve as a tool for distinguishing heat-tolerant genotypes. Linear discriminant analysis (LDA) of the spectra demonstrated a clear separation between the three genotypes in terms of the heat stress effect. Analysis of LDA coefficients identified several spectral regions that were potentially responsible for the discrimination of FTIR spectra between different genotypes and environments. These results suggest that a combination of FTIR and chemometrics can be a useful technique for characterizing the metabolic behavior of diverse wheat genotypes under heat stress.

Keywords: *Triticum aestivum* L.; FTIR spectroscopy; chemometrics; metabolomics markers; arid region; linear discriminant analysis



Citation: Osman, S.O.M.; Saad, A.S.I.; Tadano, S.; Takeda, Y.; Yamasaki, Y.; Tahir, I.S.A.; Tsujimoto, H.; Akashi, K. Probing Differential Metabolome Responses among Wheat Genotypes to Heat Stress Using Fourier Transform Infrared-Based Chemical Fingerprinting. *Agriculture* **2022**, *12*, 753. <https://doi.org/10.3390/agriculture12060753>

Academic Editor: Urs Feller

Received: 13 April 2022

Accepted: 24 May 2022

Published: 25 May 2022

Publisher's Note: MDPI stays neutral with regard to jurisdictional claims in published maps and institutional affiliations.



Copyright: © 2022 by the authors. Licensee MDPI, Basel, Switzerland. This article is an open access article distributed under the terms and conditions of the Creative Commons Attribution (CC BY) license (<https://creativecommons.org/licenses/by/4.0/>).

1. Introduction

Wheat (*Triticum aestivum* L.) is one of the most important staple crops. It contributes to the diets of humans as an important source of calories, protein, vitamins, and dietary fiber [1]. Wheat, rice, maize, and soybean contribute more than 50 percent of the calories required by the global population [2]. Among several abiotic stresses that constrain wheat production, heat stress remains one of the major challenges. Reduction in wheat yield at high temperatures is well documented [3–7]. This is expected to further escalate in the light of ensuing climate change. Intense global warming with a fast rate of global temperature increase of up to 5 °C is predicted by the end of this century [8]. Therefore, understanding the heat response of wheat is indispensable for facilitating the development of new heat-tolerant varieties.

Wheat genetic resources and their diversity have been studied extensively [9–11], and wide variation in heat stress sensitivity among genotypes has been reported [12,13]. For example, Chinese Spring has been identified as a heat-sensitive genotype [14,15], whereas Norin 61 showed heat tolerance in hot arid regions in Sudan in field studies [16,17]. The genome structures of these two genotypes have previously been reported [18]. Imam is a heat-tolerant cultivar widely grown in Sudan, regarded as the world's hottest wheat growing environment [19], and has been used as a reference genotype for detecting heat tolerance in other varieties [16].

Metabolomics is one of the omics tools used to analyze the molecular responses of plants, and has been utilized to study metabolic responses in plants under various stresses [20–22]. Metabolomics has been applied to plant breeding programs because the metabolome is arguably more closely related to the phenotype than other “omics” data [23]. Among the various technical platforms used in metabolomics, Fourier transform infrared (FTIR) spectroscopy is unique in that it provides an opportunity to study biological samples *in vivo* in a non-destructive manner [24–26], is compatible with remote sensing in the field [27,28], and allows the analysis of complex biomacromolecules such as cell wall components [29,30]. FTIR spectroscopy has been used to study the metabolome responses of plants to various environmental stresses [31–34]. In our previous study, the utilization of FTIR combined with chemometrics successfully identified spectral changes that distinguished heat-stressed and unstressed leaves in the bread wheat genotype “Norin 61” [35]. Therefore, the aim of the current study was to determine whether the FTIR spectroscopic technique is useful for characterizing the metabolome diversity of wheat genotypes with variable heat tolerance abilities. Toward this objective, three wheat genotypes, ‘Chinese Spring’, ‘Imam’, and ‘Norin 61’, with different heat tolerance levels, were used.

2. Materials and Methods

2.1. Plant Growth Condition

Seeds of wheat genotypes Chinese Spring and Imam were kindly provided by Dr. Hiroyuki Tanaka (Faculty of Agriculture, Tottori University, Tottori, Japan). Seeds of wheat genotype Norin 61 were kindly provided by Dr Yasir Serag Alnor Gorafi (Arid Land Research Center, Tottori University, Tottori, Japan). Twelve seeds each of the three wheat genotypes were placed on top of an 85-mm diameter filter paper (Filter paper type-2, Advantec, Tokyo, Japan) in a Petri dish of 90-mm diameter, and imbibed by adding 6 mL of tap water. The Petri dish was capped with a transparent lid and incubated for three days at room temperature (25 °C). Germinated seedlings were individually planted in pots containing 120 g of commercial horticulture soil (a brand “Oishii Yasaiwo Sodateru Baiyoudo,” Cainz, Honjo, Saitama, Japan). Pots were placed in a growth chamber with light/dark regimes set at 14/10 h, light intensity of approximately 500 $\mu\text{mol m}^{-2} \text{s}^{-1}$, relative humidity setting at 50%, and temperatures of 22/18 °C for the light/dark regimes. When the length of the third leaf exceeded that of the second leaf, half of the pots were transferred to a heat chamber with a daily temperature setting of 42/18 °C under light/dark regimes. In this heat chamber, the temperature was programmed to increase stepwise from 18 °C at the beginning of the light regime by 5 °C/h for 3 h, to the maximum temperature of 42 °C and maintained for 6 h. The temperature was then lowered to 33 °C for 1 h and then decreased stepwise by 5 °C/h to 18 °C in the next 3 h. Heat treatment was applied for three days, and the plants were subjected to the analyses described below.

2.2. Measurement of Canopy Temperature and Plant Growth

For the measurement of canopy temperatures, the leaf surface temperature of wheat plants at 5 h after the onset of the daily light regime was measured using a thermal camera and averaged as described previously [35]. To measure leaf length, all attached leaves of a given plant were measured using a ruler, and the values were combined. To measure shoot biomass, the aerial parts of individual plants were harvested and completely dried in an

oven (EI-450B, ETTAS, AS-ONE, Osaka, Japan) at 70 °C for three days, and the dry weight was measured.

2.3. FTIR Spectroscopy

Fully expanded third leaves of the control and the heat-treated plants were harvested and completely dried in an oven at 70 °C. The whole dried leaf (approximately 0.16 g per leaf) was placed into a 15 mL plastic tube with three stainless beads, one with 10- and the other two with 5-mm diameters, respectively, and placed into a pre-chilled aluminum block in a shaker homogenizer (Shake Master Auto, Bio Medical Science, Tokyo, Japan). The sample was ground to a fine powder at 1100 rpm for 30 min. The powdered samples (approximately 10 mg) were mixed with 1 g of powdered KBr (IR grade, Nakalai, Kyoto, Japan), and approximately 10 mg of the mixture was placed on a die of 7 mm diameter in a hydraulic press (Pixie Hydraulic Pellet Press, PIKE Technologies, Madison, WI, USA). A thin disk was formed by applying a pressure of 2.5 t cm⁻². Three disks were generated from each single plant. FTIR spectra were recorded in absorbance mode using PerkinElmer Spectrum 65 (PerkinElmer, Waltham, MA, USA) linked with Spectrum software (version 10.4.2., PerkinElmer). The spectrum was measured at mid-infrared from 4000 to 400 cm⁻¹, with a resolution of 1 cm⁻¹, and 16 scans were taken and averaged for each measurement. Each disk was measured twice; therefore, six spectra were obtained from a single plant. Six plants were used for each genotype and environmental condition; therefore, 36 spectral data points were collected for each genotype-environment combination.

2.4. Chemometrics of FTIR Spectra and Statistical Analyses

Baseline correction of FTIR spectra using a linear gradient of absorbance values between 4000 and 400 cm⁻¹ and normalization of absorbance values was performed as described previously [35]. Chemometric calculations of the FTIR spectra were performed using R statistical software [36], with a set of custom-made R scripts that were deposited in Supplementary Document S1–S7. Briefly, principal component analysis (PCA) was performed in the wavenumber region between 3600 and 400 cm⁻¹ using the *prcomp* function in the R statistics package (version 3.6.2). Calculation of the Fm biomarkers using the pair of anchor points for generating offset absorbance values was performed as described previously [35]. For linear discriminant analysis (LDA), the wavenumber region between 3600 and 400 cm⁻¹ in the 216 spectral datasets, composed of 36 spectra each from six genotype-environment combinations (3 genotypes × 2 environment), was used for the construction of an equation model using the *lda* function in the MASS package (v7.3-54). Visualizations of the resultant dataset, such as the score and loading plots in PCA, box plots in Fm biomarkers, LD1-LD2 biplot, and their scaling plots in LDA, were performed using the *ggplot2* package (v3.3.5). The Student's *t*-test was performed using the *t.test* function in R. One-way ANOVA with post-hoc Tukey HSD testing was performed using the Astatsa.com online statistical calculator (*p* < 0.05) [37].

3. Results and Discussion

3.1. Growth Response of Three Wheat Genotypes to Heat Stress

Wheat genotypes 'Chinese Spring' (CS), 'Imam', and 'Norin 61' (N61) were grown until the three-leaf stage, at a daily temperature of 22 °C, and then subjected to heat stress at a daily maximum temperature of 42 °C for three days. Canopy temperatures were significantly elevated under heat stress in all three genotypes (Figure 1A; Supplementary Table S1); the median temperatures on day 0 (hereafter referred to as C0) were in the range of 23.0–26.6 °C for the three genotypes, and on day 3 under heat stress (H3) they increased to the range of 36.6–37.1 °C. As a result, large differences in canopy temperatures between C3 and H3 were observed in these genotypes; the difference in the median temperature was 12.2, 16.3, and 13.1 °C in CS, Imam, and N61, respectively. Total leaf length was strongly suppressed under heat stress (Figure 1B; Supplementary Table S2), in which the mean values of total leaf length were decreased by 26.9, 19.7, and 13.3% in H3 plants for CS, Imam, and N61,

respectively, in comparison to their C3 counterparts. Shoot biomass also significantly decreased under stress (Figure 1C; Supplementary Table S3). The median biomass values declined by 29.8, 25.8, and 15.7% in H3 plants for CS, Imam, and N61, respectively, in comparison to their C3 counterparts. Although the N61 genotype showed a lower degree of biomass reduction, the Imam genotype still showed higher shoot biomass than the N61 genotype on day 3 of heat stress. Similarly, high biomass production by the Imam genotype in a high-temperature environment has been observed in four field environments in Sudan [17]. These observations suggest that although the degree of heat impact differed among genotypes, all genotypes showed similar growth trends in response to three days of heat stress. These growth responses were consistent with those recorded in previous studies. Gupta et al. [38] observed that heat stress resulted in the reduction of shoot length in wheat seedlings. Another study [39] showed different degrees of reduction in shoot length in different wheat seedlings under high day and night temperatures.

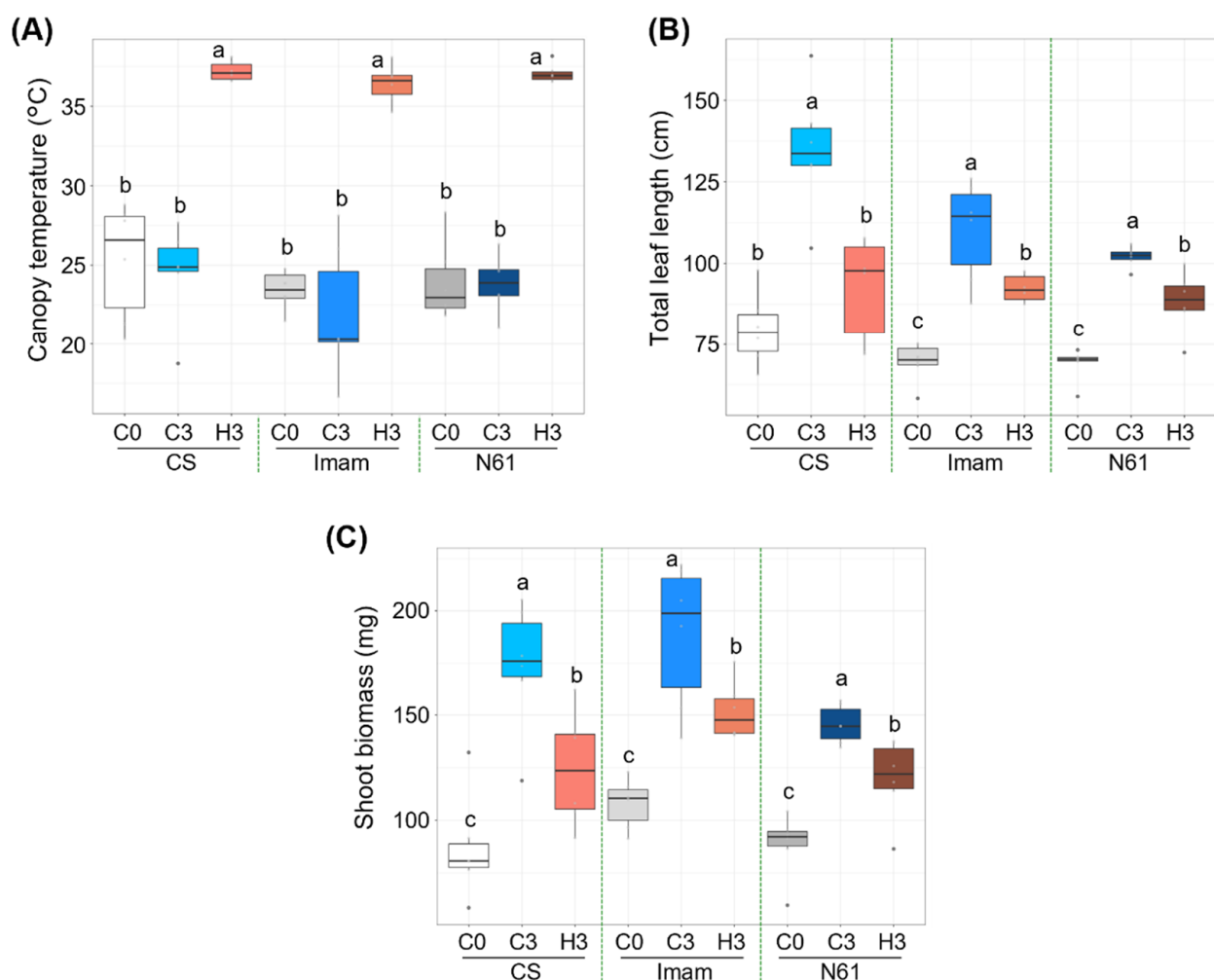


Figure 1. Effect of heat stress on the growth of wheat genotypes Chinese Spring (CS), Imam, and Norin 61 (N61). (A) Canopy temperature, (B) total leaf length, and (C) shoot biomass for (C0) before heat treatment, (C3) control plants after three days, and (H3) plants exposed to heat for three days. Six plants were used for each measurement. One-way ANOVA with post-hoc Tukey HSD test ($p < 0.05$) was carried out for statistical analysis within a given genotype.

3.2. FTIR Spectra

The fully expanded third leaves were collected from C3 and H3 plants of each genotype, and their FTIR spectra were measured. The representative spectra are shown in Figure 2. The patterns of these spectra were largely similar; a broad major peak

(3100–3600 cm^{-1}) was commonly observed in both the control and heat environments, which can be interpreted as O–H and/or N–H stretching bands [35,40–42]. Sharper peaks were observed at wavenumbers of approximately 2960 and 2925 cm^{-1} , which can be assigned to $-\text{CH}_3$ and $-\text{CH}_2-$ antisymmetric signals, respectively. No prominent peaks were observed in the 2000–2500 cm^{-1} region. A major peak was detected at approximately 1658 cm^{-1} , which can be attributed to C=C stretching, C=O stretching (amide), and N–H bending (amide I) in proteins in all genotypes in both the control and heat stress environments. All genotypes exhibited another major peak at approximately 1056 cm^{-1} , which indicated signals for C–O stretching, C–N stretching (aliphatic), and in-plane C–H bending (aromatic). All genotypes showed another broad peak at approximately 618 cm^{-1} , which can be interpreted as =C–H out-of-plane bending, =C–H bending, or C–S stretching signals. However, as shown in Figure 2, definite differences between genotypes and environments were not evident to the naked eye, raising the necessity of applying further chemometrics analysis to the FTIR data, as in previous studies [35,43–45].

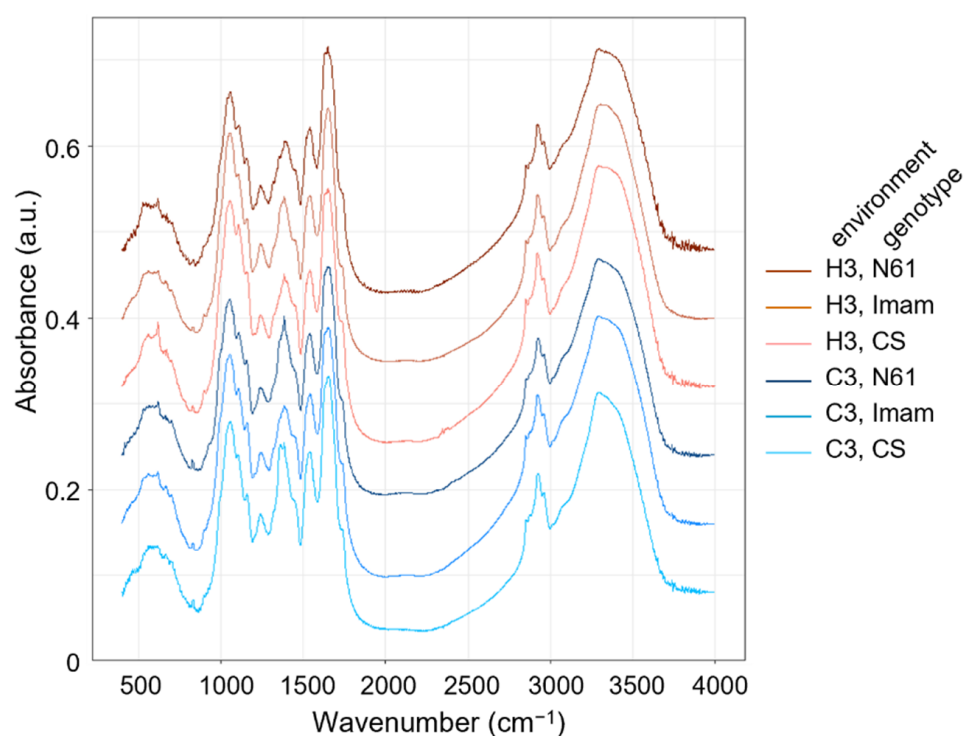


Figure 2. Representative FTIR spectra in the leaves of wheat genotypes Chinese Spring (CS), Imam, and Norin 61 (N61). Spectra drawn in blue and red color series represent those for control (C3) and heat stress environments (H3), respectively.

3.3. Principal Component Analysis

To characterize the spectral patterns of the three wheat genotypes under the C3 and H3 environments, principal component analysis (PCA) was performed. The PC1–PC2 score plot, which explained 76.2% of total variation (Supplementary Figure S1A), showed partial separation between genotypes and environments (Figure 3). For instance, the C3–CS spectra were mostly clustered in the PC2 negative range from -25 to -50 , whereas the H3–CS counterparts tended to be positioned at higher PC2 values. The C3–Imam spectra were widely scattered in the PC1 positive range of $+40$ to $+100$, whereas their H3 counterparts were mostly situated at lower PC1 values between -20 and $+30$. The C3–N61 spectra were mostly situated in the PC1 range between -80 and $+20$, and PC2 ranged between -10 and $+20$, while their H3 counterparts were mostly spread around the -130 to $+10$ PC1 range and the -10 to $+45$ PC2 range. Their loading plots showed a complex pattern over the entire range of 400–3600 cm^{-1} (Supplementary Figure S1B–D). However, overlapping distributions of different genotypes and environmental conditions were also evident in the

PC1–PC2 score plot, suggesting the necessity of applying other chemometrics techniques to characterize their spectral features.

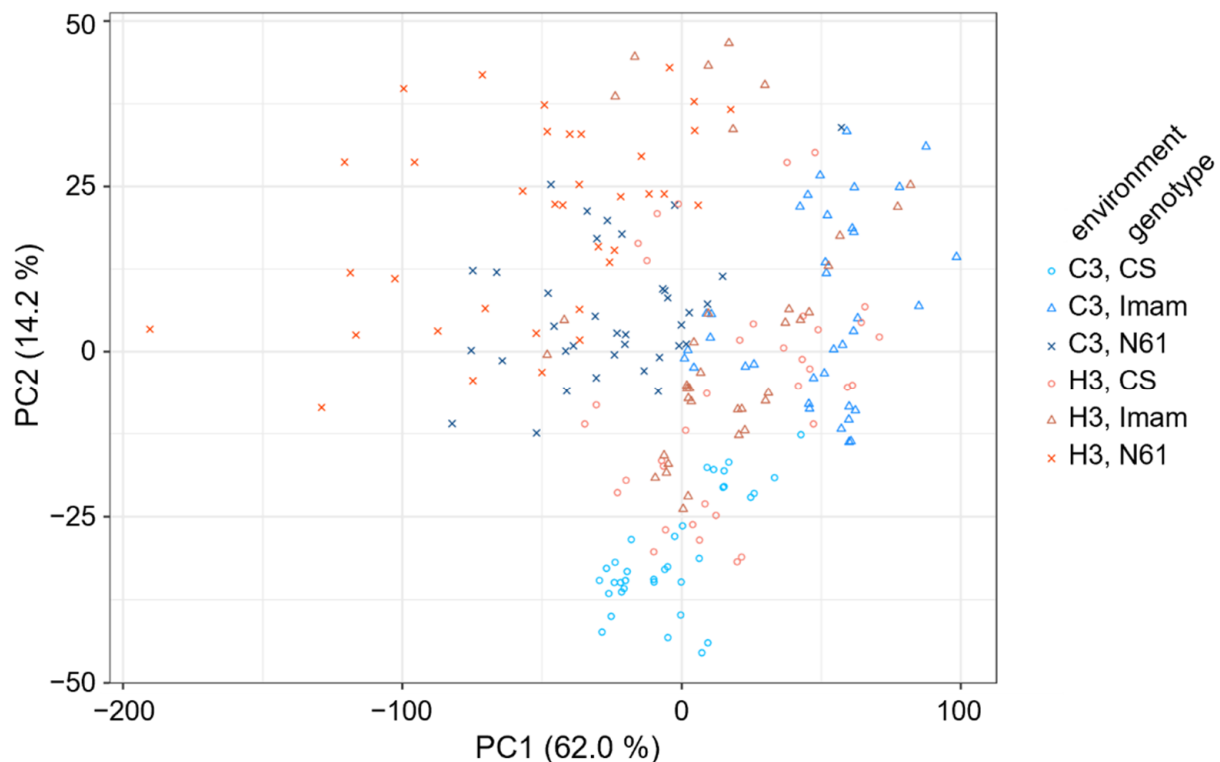


Figure 3. Score plot of principal component analysis showing the distribution of FTIR spectra for three wheat genotypes under two environmental conditions. Symbols for the three genotypes and two environments are shown at the right of the panel.

3.4. Behavior of FTIR Biomarkers

In our previous study [35], six FTIR-based biomarkers, Fm482, Fm576, Fm1251, Fm1465, Fm1502, and Fm1729 (Supplementary Table S4), were developed to distinguish between control and heat-stressed leaves in N61 genotype. These markers were based on the offset absorbance values at specific wavenumbers and were calculated using the absorbance of the two anchor wavenumbers in the vicinity of the target wavenumber. Applying these markers to the FTIR spectra in this study showed similar responses for some markers between different genotypes (Figure 4; Supplementary Table S4). Markers Fm482 and Fm1502 were reduced in all genotypes (Figure 4A,E), suggesting a common chemical change between these genotypes. Wavenumber 482 cm^{-1} , a target wavenumber for the marker Fm482, was located outside the “fingerprinting region” and was related to a methoxy group ($472/475\text{ cm}^{-1}$) [41] and S–S stretching ($450\text{--}550\text{ cm}^{-1}$) [40]. The latter may be related to the heat-induced protein disulfide isomerase in wheat genotype Jing411 [46], which catalyzes covalent cross-linking of sulfhydryl groups of cysteine residues, thereby stabilizing the structure of cellular proteins under heat stress. The Fm1502 marker is related to lignin [47,48], suggesting that physicochemical changes in cell wall components may occur under heat stress in these wheat genotypes, as has been observed in coffee leaves [48].

Other markers, in contrast, showed differential behaviors between genotypes. The Fm1465 marker, which may be associated with suberin/cutin, lipids, and/or cell wall polysaccharides [35,40,49–52], increased under heat stress in CS and N61, but decreased in the Imam genotype (Figure 4D). The Fm576 marker increased under heat stress in CS, but decreased in N61, and was statistically unchanged in Imam (Figure 4B). Information on the assignment of the wavenumber 576 cm^{-1} to chemical structures has remained relatively scarce [41], except for carbon–halogen stretching ($400\text{--}800\text{ cm}^{-1}$), P=S stretching

(500–850 cm^{-1}), and P–Cl stretching (300–600 cm^{-1}) [40]. Nevertheless, these observations suggested that biochemical responses to heat stress may be largely different between these genotypes.

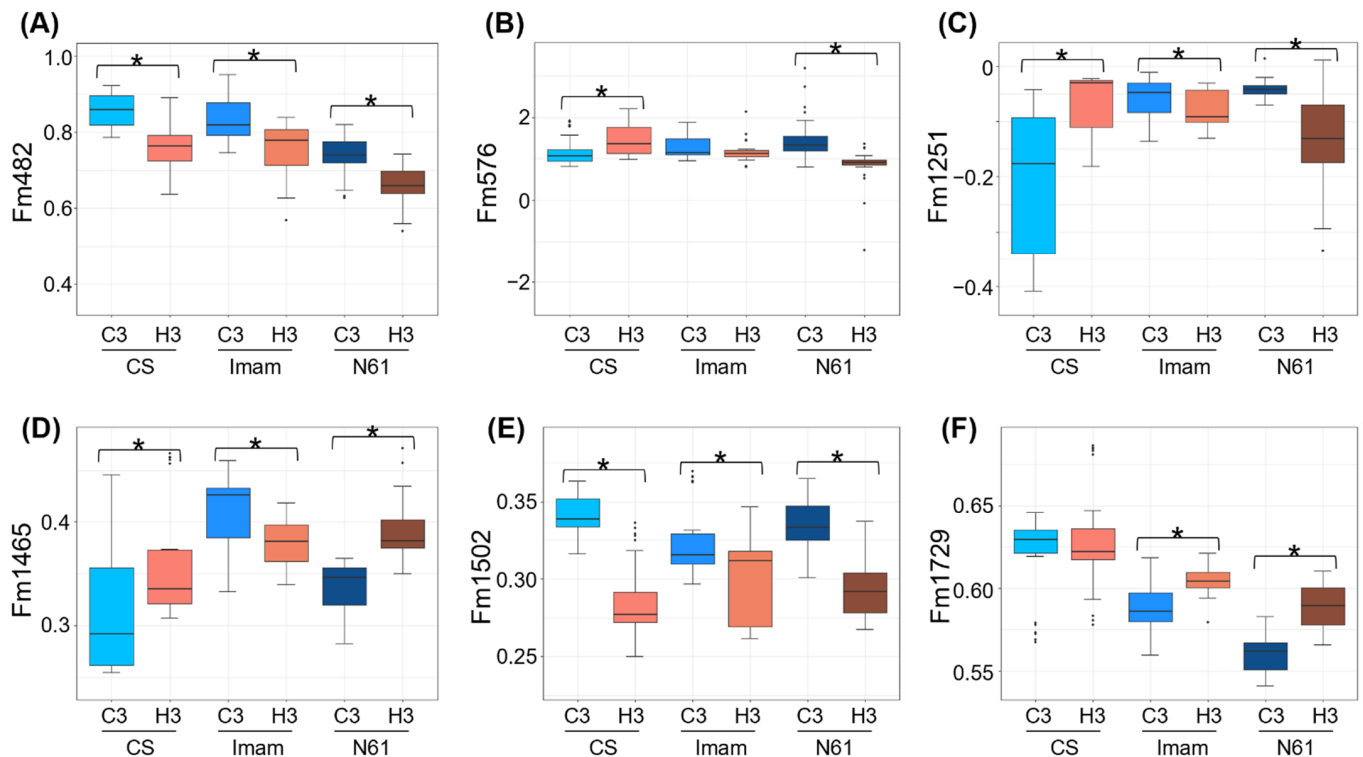


Figure 4. Comparison of FTIR-based biomarkers under heat stress between the three genotypes tested. Boxplots for (A) Fm482, (B) Fm576, (C) Fm1251, (D) Fm1465, (E) Fm1502, and (F) Fm1729 are shown for CS, Imam, and N61 genotypes under C3 and H3 environments. The 36 spectra included each genotype–environment combination. Asterisks represent statistically significant differences at $p < 0.01$.

Interestingly, behaviors of the markers Fm1251 and Fm1729 were different between heat-tolerant and -susceptible genotypes (Figure 4C,F). The Fm1251 marker, which is related to hemicellulose and/or pectin [35,40,53], decreased under heat stress in the heat-tolerant Imam and N61 genotypes, while an increase was observed in the heat-sensitive CS genotype (Figure 4C). This observation may suggest that chemical changes in the extracellular matrix, which potentially functions as a regulator for cell wall porosity and heat conductance [48,54], are contrastingly different between heat-tolerant and -susceptible genotypes. The Fm1729 marker, which is located in the carbonyl ester region (1720–1760 cm^{-1}) and/or its oxidized derivatives [32,35,40–42,55,56], was increased under heat stress in heat-tolerant Imam and N61 genotypes, whereas the value was unchanged in the heat-susceptible CS genotype (Figure 4F). This spectral region provides information on the polar interfacial regions of pectin or membrane lipids [32,55]. The latter is consistent with a previous report that heat-tolerant and -susceptible wheat genotypes showed differential lipidome responses under stress [57]. Therefore, the markers Fm1251 and Fm1729 may potentially serve as tools for distinguishing heat-tolerant and -susceptible wheat genotypes.

3.5. Linear Discriminant Analysis

Linear discriminant analysis (LDA) was performed to further characterize the FTIR spectral differences between the different genotypes. The 216 FTIR spectra forming six classes (three genotypes \times two environments) were used to construct the LDA model. The proportion of trace values for the resultant five discriminant functions (LDs) showed that the first two LDs (LD1 and LD2) accounted for 48.2 and 24.5% of total variance, respectively

(Supplementary Figure S2). The first two LDs were used to draw a graphical distribution of each spectrum, which showed six distinct clusters for each ‘genotype × environment’ class in the scatter plot (Figure 5). The plot shows a typical feature of LDA, which maximizes between-class variance while minimizing within-class variance [58,59]. The following features were recognized from the LD1–LD2 scatter plot: (i) Classes for the same genotypes were located in closer positions. For example, two classes (C3 and H3) for the Imam genotype were located in the region spanning from -28 to 6 for LD1, and from -42 to -21 for LD2 coordinates (Figure 5), which may suggest the presence of genotype-specific features in the FTIR spectra. The ability of FTIR to discriminate between different genotypes is not unique to this study, and has been reported previously in many studies, including grapevine genotypes [60] and geographical classification of coffee [61]. (ii) In all genotypes, clusters for the heat stress environment were situated in higher LD1 ranges in comparison to their control counterparts, indicating that LD1 may be associated with the presence or absence of heat stress. (iii) In C3 and N61 genotypes, the LD2 values for heat stress clusters were shifted downward from their control counterparts, whereas an opposite upward shift of the heat cluster was observed in the Imam genotype, suggesting that LD2 may partially reflect genotype-specific heat responses.

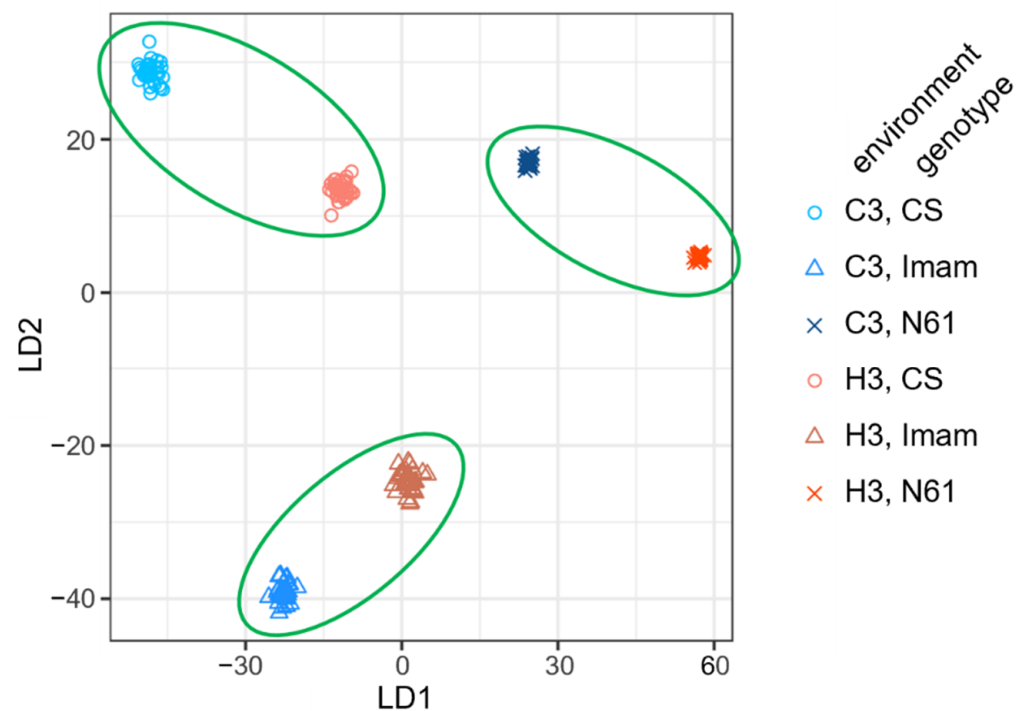


Figure 5. Scatter plot of LD1 and LD2 derived from the linear discriminant analysis (LDA). The LDs are the discriminate functions of the LDA model. Each point represents the LD1–LD2 coordinate for each FTIR spectrum. Symbols for the three genotypes and two environmental conditions are shown at the right of the panel. Green ellipses denote the location of each wheat genotype.

To obtain information on the influential wavenumber regions in the FTIR spectra for discriminating different genotypes and environmental conditions, the coefficients of the LDs for each wavenumber were examined. The coefficient of LDs, or scaling value, indicates the loading or contribution of each wavenumber to the LD function, in such a way that higher absolute values of coefficients potentially show greater contribution to the discrimination [62]. A two-dimensional scatter plot of the coefficients showed that most of the wavenumbers were loosely clustered in the origin of the LD1–LD2 plain, whereas a considerable quantity of ‘characteristic’ wavenumbers deviated from the center (Figure 6A). One-dimensional plots of coefficients for either LD1 or LD2 versus wavenumbers revealed that several spectral regions, i.e., $400\text{--}800\text{ cm}^{-1}$, $1200\text{--}1300\text{ cm}^{-1}$, $1450\text{--}1550\text{ cm}^{-1}$, and

1700–1800 cm^{-1} regions, had strong absolute values for either LD1 or LD2 (Figure 6B,C), suggesting that these regions may have major contributions to the spectral discrimination of different genotypes and environmental conditions. These regions include the 600–1500 cm^{-1} region that has been referred to as the “fingerprinting” region in which infrared absorption is cumulatively influenced by small steric or electronic effects depending on the nature of the molecules [63]. The most ‘characteristic’ wavenumbers that deviated from the origin of the LD1–LD2 plain (Figure 6A) were predominantly located in the ranges of 400–500 cm^{-1} and 1200–1300 cm^{-1} . The 400–500 cm^{-1} range was situated in the ascending curve from the spectral margin of 400 cm^{-1} which was used for baseline correction, thus showing lower absorbance values (hence, it should have a lower contribution to discrimination). Moreover, this region suffered from a jagged shaped spectral curve, which was probably derived from noise (Supplementary Figure S3). Therefore, in the subsequent analysis, we focused on the 1200–1300 cm^{-1} region, which is within the fingerprinting region and potentially contains signals from multiple functional groups, such as C–O stretching, in-plane C–H bending (aromatic), and aliphatic C–O stretching [40,41].

To gain insight into the features of the 1200–1300 cm^{-1} region, averaged FTIR spectral curves for this region were compared among genotypes and environments (Figure 7). This region contained four characteristic wavenumbers: 1222 cm^{-1} (LD1 coefficient of +0.247), 1256 cm^{-1} (LD1 coefficient of –0.262), 1204 (LD2 coefficient of +0.184), and 1290 cm^{-1} (LD2 coefficient of –0.235) (Figure 6A). The averaged FTIR curves showed that the wavenumbers 1222 cm^{-1} and 1256 cm^{-1} were situated in the middle of the ascending and descending curves, respectively, to a peak centered at 1241 cm^{-1} , which has been tentatively identified as C–O stretching, in-plane C–H bending (aromatic), and aliphatic C–O stretching signals [24]. The absorbance values at these wavenumbers for the six environment \times genotype combinations were in descending order of C3–CS, C3–Imam, H3–CS, H3–Imam, C3–N61, and H3–N61 (Figure 7), which showed an association with the ascending order of LD1 scores in LDA (Figure 5). This was consistent with the negative LD1 coefficient value for the wavenumber 1256 cm^{-1} , but showed an opposite trend to the positive LD1 coefficient for the wavenumber 1222 cm^{-1} . Although the reason for this discrepancy is currently unknown, one possibility is that the 1222 cm^{-1} variable may counteract the 1256 cm^{-1} variable to minimize the within-class variance in the LDA scores, which is a basic characteristic of LDA [58,59]. Another possible factor is that each wavenumber may exert rather small effects, and cumulative actions of multiple wavenumbers are required for the final discrimination. Similar trends were observed for wavenumbers 1204 cm^{-1} (negative LD2 coefficient) and 1290 cm^{-1} (positive LD2 coefficient), in which the absorbance values were only partially correlated with the LD2 score (Figures 5 and 7). Overall, these observations suggest that further studies are needed to fully elucidate spectral behavior and underlying biochemical changes during heat stress in a variety of wheat genotypes.

In this study, utility of FTIR-based chemical fingerprinting in combination with chemometrics was demonstrated, for characterizing metabolome responses to heat stress in three genotypes of bread wheat with different heat tolerances. Application of this technique in future will benefit the study of responses to other types of abiotic stresses, such as drought stress and drought–heat combination in various wheat genotypes with different water demands [13,64,65].

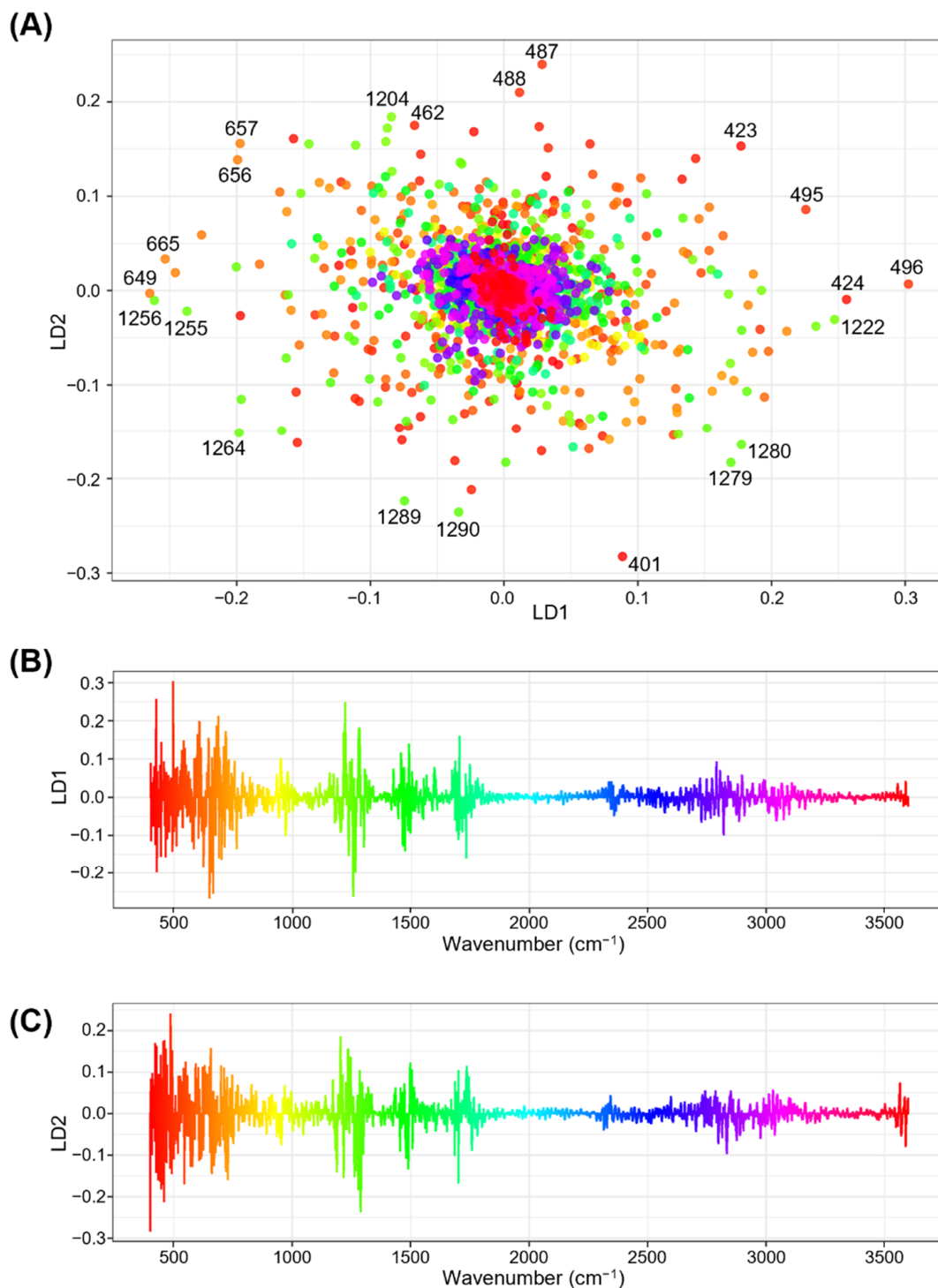


Figure 6. Relationships between the coefficients of the first two linear discriminants (LD1 and LD2) and wavenumbers in linear discriminant analysis (LDA). (A) Two-dimensional scatter plot for the coefficients of linear discriminant LD1 and LD2. Respective points represent the wavenumbers from 400 to 4000 cm^{-1} . Assignment of color gradients to respective wavenumbers are the same as those presented in (B,C). Numbers in black font at respective color points designate wavenumbers for characteristic data points with higher absolute coefficient values (B,C). One-dimensional column plots showing relationships between wavenumbers and coefficients of (B) LD1 and (C) LD2. The coefficient values for each wavenumber are expressed using a rainbow color gradient along their x -axes.

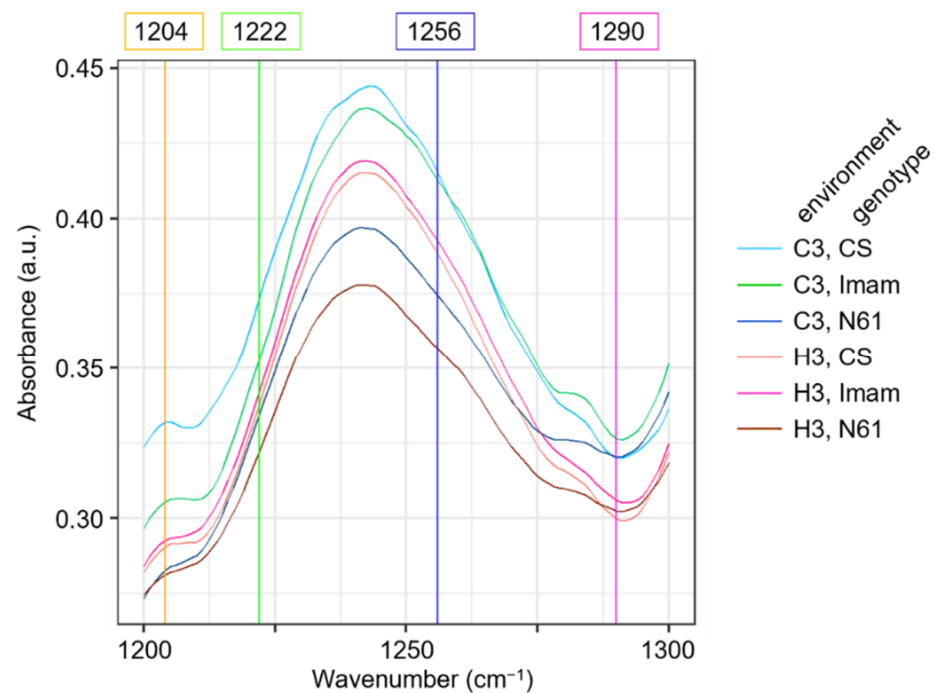


Figure 7. Magnified view of averaged FTIR spectra in the wavenumber range from 1200 to 1300 cm^{-1} for strong discriminatory variable wavenumbers detected in LDA. Averaged spectra for six wheat genotypes \times environment combinations are shown, according to the legend depicted on the right. Colored vertical straight lines and their numbers on top of the panel denote characteristic wavenumbers detected in LDA as strong discriminatory variables.

4. Conclusions

The PCA, spectral biomarker assays, and LDA of FTIR spectra demonstrated the existence of common and distinct metabolic responses between the three genotypes of bread wheat with different heat tolerances. The spectral biomarker assay showed that Fm1251 and Fm1729 markers potentially discriminate heat-tolerant and -susceptible genotypes, suggesting that these markers may serve as a selection tool for heat-tolerant genotypes. LDA of the coefficient values indicated the presence of potential discriminatory spectral regions that were associated with genotype-specific metabolic responses. The present study demonstrates the versatility and potential of the FTIR fingerprinting technique for elucidating the diversity of metabolic behaviors among diverse plant resources.

Supplementary Materials: The following supporting information can be downloaded at: <https://www.mdpi.com/article/10.3390/agriculture12060753/s1>. Table S1: One-way ANOVA with post-hoc Tukey HSD test on canopy temperature; Table S2: One-way ANOVA with post-hoc Tukey HSD test on total leaf length; Table S3: One-way ANOVA with post-hoc Tukey HSD test on shoot biomass; Table S4: Characteristics of spectral markers; Figure S1: Supplementary data on the PCA of FTIR spectra; Figure S2: Values of proportion of trace in linear discriminant analysis; Figure S3: Magnified view of averaged FTIR spectra in the wavenumber ranges from 400 to 510 cm^{-1} that detected strong discriminatory variable wavenumbers in LDA; Document S1: R-scripts for the processing of FT-IR data.

Author Contributions: Conceptualization, S.O.M.O., A.S.I.S. and K.A.; methodology, S.O.M.O., S.T., Y.T. and K.A.; investigation, S.O.M.O.; software, S.O.M.O., S.T. and K.A.; validation, A.S.I.S., Y.Y., I.S.A.T., H.T. and K.A.; writing—original draft preparation, S.O.M.O.; writing—review and editing, A.S.I.S., Y.Y., I.S.A.T., H.T. and K.A.; supervision, A.S.I.S., I.S.A.T., H.T. and K.A.; project administration, I.S.A.T. and H.T.; funding acquisition, I.S.A.T. and H.T. All authors have read and agreed to the published version of the manuscript.

Funding: This research was partially funded by the Science and Technology Research Partnership for Sustainable Development (SATREPS, JPMJSA1805) by JST and JICA, the Joint Research Program and the Project Marginal Region Agriculture, the Arid Land Research Center, Tottori University, the IPDRE Program, Tottori University, and the Republic of Sudan.

Institutional Review Board Statement: Not applicable.

Informed Consent Statement: Not applicable.

Data Availability Statement: Not applicable.

Acknowledgments: The authors thank Hiroyuki Tanaka and Yasir Serag Alnor Gorafi for providing the wheat seed materials. The authors thank the technicians and colleagues at the Molecular and Cellular Biology Laboratory at Tottori University.

Conflicts of Interest: The authors declare no conflict of interest.

References

- Shewry, P.R.; Hey, S.J. The contribution of wheat to human diet and health. *Food Energy Secur.* **2015**, *4*, 178–202. [[CrossRef](#)] [[PubMed](#)]
- Zhao, C.; Liu, B.; Piao, S.; Wang, X.; Lobell, D.B.; Huang, Y.; Huang, M.; Yao, Y.; Bassu, S.; Ciais, P.; et al. Temperature increase reduces global yields of major crops in four independent estimates. *Proc. Natl. Acad. Sci. USA* **2017**, *114*, 9326–9331. [[CrossRef](#)] [[PubMed](#)]
- Mitchell, R.A.C.; Mitchell, V.J.; Driscoll, S.P.; Franklin, J.; Lawlor, D.W. Effects of increased CO₂ concentration and temperature on growth and yield of winter wheat at two levels of nitrogen application. *Plant Cell Environ.* **1993**, *16*, 521–529. [[CrossRef](#)]
- Stone, P.J.; Nicolas, M.E. Effect of timing of heat stress during grain filling on two wheat varieties differing in heat tolerance. I. grain growth. *Funct. Plant Physiol.* **1995**, *22*, 927–934. [[CrossRef](#)]
- Semenov, M.A.; Halford, N.G. Identifying target traits and molecular mechanisms for wheat breeding under a changing climate. *J. Exp. Bot.* **2009**, *60*, 2791–2804. [[CrossRef](#)] [[PubMed](#)]
- Schittenhelm, S.; Langkamp-Wedde, T.; Kraft, M.; Kottmann, L.; Matschiner, K. Effect of two-week heat stress during grain filling on stem reserves, senescence, and grain yield of European winter wheat cultivars. *J. Agron. Crop Sci.* **2020**, *206*, 722–733. [[CrossRef](#)]
- Matsunaga, S.; Yamasaki, Y.; Toda, Y.; Mega, R.; Akashi, K.; Tsujimoto, H. Stage-specific characterization of physiological response to heat stress in the wheat cultivar Norin 61. *Int. J. Mol. Sci.* **2021**, *22*, 6942. [[CrossRef](#)]
- Solomon, S.; Qin, D.; Manning, M.; Marquis, M.; Averyt, K.; Tignor, M.M.B.; LeRoy Miller, H.; Chen, Z. *Climate Change 2007: The Physical Science Basis. Contribution of Working Group I to the Fourth Assessment Report of the Intergovernmental Panel on Climate Change*; Cambridge University Press: New York, NY, USA, 2007.
- Reif, J.C.; Zhang, P.; Dreisigacker, S.; Warburton, M.L.; van Ginkel, M.; Hoisington, D.; Bohn, M.; Melchinger, A.E. Wheat genetic diversity trends during domestication and breeding. *Theor. Appl. Genet.* **2005**, *110*, 859–864. [[CrossRef](#)]
- Gorafi, Y.S.A.; Kim, J.-S.; Elbashir, A.A.E.; Tsujimoto, H. A population of wheat multiple synthetic derivatives: An effective platform to explore, harness and utilize genetic diversity of *Aegilops tauschii* for wheat improvement. *Theor. Appl. Genet.* **2018**, *131*, 1615–1626. [[CrossRef](#)]
- Balfourier, F.; Bouchet, S.; Robert, S.; de Oliveira, R.; Rimbart, H.; Kitt, J.; Choulet, F.; Paux, E. Worldwide phylogeography and history of wheat genetic diversity. *Sci. Adv.* **2019**, *5*, eaav0536. [[CrossRef](#)]
- Tadesse, W.; Sanchez-Garcia, M.; Assefa, S.G.; Amri, A.; Bishaw, Z.; Ogbonnaya, F.C.; Baum, M. Genetic gains in wheat breeding and its role in feeding the world. *Crop Breed. Genet. Genomics* **2019**, *1*, e190005. [[CrossRef](#)]
- Qaseem, M.F.; Qureshi, R.; Shaheen, H. Effects of pre-anthesis drought, heat and their combination on the growth, yield and physiology of diverse wheat (*Triticum aestivum* L.) genotypes varying in sensitivity to heat and drought stress. *Sci. Rep.* **2019**, *9*, 6955. [[CrossRef](#)] [[PubMed](#)]
- Wang, X.; Hou, L.; Lu, Y.; Wu, B.; Gong, X.; Liu, M.; Wang, J.; Sun, Q.; Vierling, E.; Xu, S. Metabolic adaptation of wheat grain contributes to a stable filling rate under heat stress. *J. Exp. Bot.* **2018**, *69*, 5531–5545. [[CrossRef](#)] [[PubMed](#)]
- Qin, D.; Wu, H.; Peng, H.; Yao, Y.; Ni, Z.; Li, Z.; Zhou, C.; Sun, Q. Heat stress-responsive transcriptome analysis in heat susceptible and tolerant wheat (*Triticum aestivum* L.) by using Wheat Genome Array. *BMC Genomics* **2008**, *9*, 432. [[CrossRef](#)]
- Elbashir, A.A.E.; Gorafi, Y.S.A.; Tahir, I.S.A.; Kim, J.S.; Tsujimoto, H. Wheat multiple synthetic derivatives: A new source for heat stress tolerance adaptive traits. *Breed. Sci.* **2017**, *67*, 248–256. [[CrossRef](#)] [[PubMed](#)]
- Elbashir, A.A.; Gorafi, Y.S.; Tahir, I.S.; Elhashimi, A.M.; Abdalla, M.G.; Tsujimoto, H. Genetic variation in heat tolerance-related traits in a population of wheat multiple synthetic derivatives. *Breed. Sci.* **2017**, *67*, 483–492. [[CrossRef](#)] [[PubMed](#)]
- Walkowiak, S.; Gao, L.; Monat, C.; Haberer, G.; Kassa, M.T.; Brinton, J.; Ramirez-Gonzalez, R.H.; Kolodziej, M.C.; Delorean, E.; Thambugala, D.; et al. Multiple wheat genomes reveal global variation in modern breeding. *Nature* **2020**, *588*, 277–283. [[CrossRef](#)]
- Iizumi, T.; Ali-Babiker, I.E.A.; Tsubo, M.; Tahir, I.S.; Kurosaki, Y.; Kim, W.; Gorafi, Y.S.; Idris, A.A.; Tsujimoto, H. Rising temperature and increasing demand challenge wheat supply in Sudan. *Nat. Food* **2021**, *2*, 19–27. [[CrossRef](#)]

20. Ghatak, A.; Chaturvedi, P.; Weckwerth, W. Metabolomics in plant stress physiology. In *Plant Genetics and Molecular Biology; Advances in Biochemical Engineering/Biotechnology Book Series*; Springer: Berlin/Heidelberg, Germany, 2018; pp. 187–236. [[CrossRef](#)]
21. Hamany Djande, C.Y.; Pretorius, C.; Tugizimana, F.; Piater, L.A.; Dubery, I.A. Metabolomics: A tool for cultivar phenotyping and investigation of grain crops. *Agronomy* **2020**, *10*, 831. [[CrossRef](#)]
22. Matsunaga, S.; Yamasaki, Y.; Mega, R.; Toda, Y.; Akashi, K.; Tsujimoto, H. Metabolome profiling of heat priming effects, senescence, and acclimation of bread wheat induced by high temperatures at different growth stages. *Int. J. Mol. Sci.* **2021**, *22*, 13139. [[CrossRef](#)]
23. Sakurai, N. Recent applications of metabolomics in plant breeding. *Breed. Sci.* **2022**, *72*, 56–65. [[CrossRef](#)]
24. Bouyanfif, A.; Liyanage, S.; Hewitt, J.E.; Vanapalli, S.A.; Moustaid-Moussa, N.; Hequet, E.; Abidi, N. FTIR imaging detects diet and genotype-dependent chemical composition changes in wild type and mutant *C. elegans* strains. *Analyst* **2017**, *142*, 4727–4736. [[CrossRef](#)] [[PubMed](#)]
25. Munz, E.; Rolletschek, H.; Oeltze-Jafra, S.; Fuchs, J.; Guendel, A.; Neuberger, T.; Ortleb, S.; Jakob, P.M.; Borisjuk, L. A functional imaging study of germinating oilseed rape seed. *New Phytol.* **2017**, *216*, 1181–1190. [[CrossRef](#)] [[PubMed](#)]
26. Petrou, K.; Nielsen, D.A.; Heraud, P. Single-cell biomolecular analysis of coral algal symbionts reveals opposing metabolic responses to heat stress and expulsion. *Front. Mar. Sci.* **2018**, *5*, 110. [[CrossRef](#)]
27. Li, H.; Liu, Z.; Mamtimin, A.; Liu, J.; Liu, Y.; Ju, C.; Zhang, H.; Gao, Z. A new linear relation for estimating surface broadband emissivity in arid regions based on FTIR and MODIS products. *Remote Sens.* **2021**, *13*, 1686. [[CrossRef](#)]
28. Yalkun, A.; Mamtimin, A.; Liu, S.; Yang, F.; He, Q.; Qi, F.; Liu, Y. Coefficients optimization of the GLASS broadband emissivity based on FTIR and MODIS data over the Taklimakan Desert. *Sci. Rep.* **2019**, *9*, 18460. [[CrossRef](#)] [[PubMed](#)]
29. McCann, M.C.; Chen, L.; Roberts, K.; Kemsley, E.K.; Sene, C.; Carpita, N.C.; Stacey, N.J.; Wilson, R.H. Infrared microspectroscopy: Sampling heterogeneity in plant cell wall composition and architecture. *Physiol. Plant.* **1997**, *100*, 729–738. [[CrossRef](#)]
30. Liu, X.; Renard, C.M.; Bureau, S.; Le Bourvellec, C. Revisiting the contribution of ATR-FTIR spectroscopy to characterize plant cell wall polysaccharides. *Carbohydr. Polym.* **2021**, *262*, 117935. [[CrossRef](#)]
31. Zhao, X.; Yang, X.; Shi, Y.; Chen, G.; Li, X. Protein and lipid characterization of wheat roots plasma membrane damaged by Fe and H₂O₂ using ATR-FTIR method. *J. Biophys. Chem.* **2013**, *4*, 28–35. [[CrossRef](#)]
32. Lahlali, R.; Jiang, Y.; Kumar, S.; Karunakaran, C.; Liu, X.; Borondics, F.; Hallin, E.; Bueckert, R. ATR-FTIR spectroscopy reveals involvement of lipids and proteins of intact pea pollen grains to heat stress tolerance. *Front. Plant Sci.* **2014**, *5*, 747. [[CrossRef](#)]
33. Westworth, S.; Ashwath, N.; Cozzolino, D. Application of FTIR-ATR spectroscopy to detect salinity response in beauty leaf tree (*Calophyllum inophyllum* L.). *Energy Proc.* **2019**, *160*, 761–768. [[CrossRef](#)]
34. Nikalje, G.C.; Kumar, J.; Nikam, T.D.; Suprasanna, P. FT-IR profiling reveals differential response of roots and leaves to salt stress in a halophyte *Sesuvium portulacastrum* (L.) L. *Biotechnol. Rep.* **2019**, *23*, e00352. [[CrossRef](#)] [[PubMed](#)]
35. Osman, S.O.M.; Saad, A.S.I.; Tadano, S.; Takeda, Y.; Konaka, T.; Yamasaki, Y.; Tahir, I.S.A.; Tsujimoto, H.; Akashi, K. Chemical fingerprinting of heat stress responses in the leaves of common wheat by Fourier transform infrared spectroscopy. *Int. J. Mol. Sci.* **2022**, *23*, 2842. [[CrossRef](#)] [[PubMed](#)]
36. R Core Team. *A Language and Environment for Statistical Computing*; R Foundation for Statistical Computing: Vienna, Austria, 2020. Available online: <http://www.r-project.org/index.html> (accessed on 1 October 2020).
37. Astatsa. Complex Online Web Statistics Calculator. Available online: <https://astatsa.com/> (accessed on 3 April 2022).
38. Gupta, N.K.; Agarwal, S.; Agarwal, V.P.; Nathawat, N.S.; Gupta, S.; Singh, G. Effect of short-term heat stress on growth, physiology and antioxidative defense system in wheat seedlings. *Acta Physiol. Plant.* **2013**, *35*, 1837–1842. [[CrossRef](#)]
39. Keleş, Y.; Öncel, I. Response of antioxidative defense system to temperature and water stress combinations in wheat seedlings. *Plant Sci.* **2002**, *163*, 783–790. [[CrossRef](#)]
40. Stuart, B. Biological Application. In *Infrared Spectroscopy: Fundamentals and Applications*; Stuart, B., Ed.; John Wiley & Sons Ltd.: Chichester, UK, 2004; pp. 137–165.
41. Talari, A.C.S.; Martinez, M.A.G.; Movasaghi, Z.; Rehman, S.; Rehman, I.U. Advances in Fourier transform infrared (FTIR) spectroscopy of biological tissues. *Appl. Spectrosc. Rev.* **2016**, *52*, 456–506. [[CrossRef](#)]
42. Kamnev, A.A.; Dyatlova, Y.A.; Kenzhegulov, O.A.; Vladimirova, A.A.; Mamchenkova, P.V.; Tugarova, A.V. Fourier transform infrared (FTIR) spectroscopic analyses of microbiological samples and biogenic selenium nanoparticles of microbial origin: Sample preparation effects. *Molecules* **2021**, *26*, 1146. [[CrossRef](#)]
43. Ami, D.; Natalello, A.; Mereghetti, P.; Neri, T.; Zanoni, M.; Monti, M.; Doglia, S.M.; Redi, C.A. FT-IR spectroscopy supported by PCA-LDA analysis for the study of embryonic stem cell differentiation. *Spectroscopy* **2010**, *24*, 89–97. [[CrossRef](#)]
44. Christou, C.; Agapiou, A.; Kokkinofa, R. Use of FTIR spectroscopy and chemometrics for the classification of carobs origin. *J. Adv. Res.* **2018**, *10*, 1–8. [[CrossRef](#)]
45. Tarapoulouzi, M.; Kokkinofa, R.; Theocharis, C.R. Chemometric analysis combined with FTIR spectroscopy of milk and Halloumi cheese samples according to species' origin. *Food Sci. Nutr.* **2020**, *8*, 3262–3273. [[CrossRef](#)]
46. Zhang, Y.; Pan, J.; Huang, X.; Guo, D.; Lou, H.; Hou, Z.; Su, M.; Liang, R.; Xie, C.; You, M.; et al. Differential effects of a post-anthesis heat stress on wheat (*Triticum aestivum* L.) grain proteome determined by iTRAQ. *Sci. Rep.* **2017**, *7*, 3468. [[CrossRef](#)]
47. Kurian, J.K.; Garipey, Y.; Orsat, V.; Raghavan, V. Microwave-assisted lime treatment and recovery of lignin from hydrothermally treated sweet sorghum bagasse. *Biofuels* **2015**, *6*, 341–355. [[CrossRef](#)]

48. Lima, R.B.; dos Santos, T.B.; Vieira, L.G.E.; Ferrarese, M.L.L.; Ferrarese-Filho, O.; Donatti, L.; Boeger, M.R.T.; Petkowicz, C.L.O. Heat stress causes alterations in the cell-wall polymers and anatomy of coffee leaves (*Coffea arabica* L.). *Carbohydr. Polym.* **2013**, *93*, 135–143. [[CrossRef](#)] [[PubMed](#)]
49. Stewart, D. Fourier transform infrared microspectroscopy of plant tissues. *Appl. Spectrosc.* **1996**, *50*, 357–365. [[CrossRef](#)]
50. Lammers, K.; Arbuckle-Keil, G.; Dighton, J. FTIR study of the changes in carbohydrate chemistry of three New Jersey pine barrens leaf litters during simulated control burning. *Soil Biol. Biochem.* **2009**, *41*, 340–347. [[CrossRef](#)]
51. Stuart, B. *Biological Applications of Infrared Spectroscopy*; ACO Series; Wiley: Chichester, UK, 1997.
52. Gorgulu, S.T.; Dogan, M.; Severcan, F. The characterization and differentiation of higher plants by Fourier transform infrared spectroscopy. *Appl. Spectrosc.* **2007**, *61*, 300–308. [[CrossRef](#)] [[PubMed](#)]
53. Mascarenhas, M.; Dighton, J.; Arbuckle, G.A. Characterization of plant carbohydrates and changes in leaf carbohydrate chemistry due to chemical and enzymatic degradation measured by microscopic ATR FTIR spectroscopy. *Appl. Spectrosc.* **2000**, *54*, 681–686. [[CrossRef](#)]
54. Baron-Epel, O.; Gharyal, P.K.; Schindler, M. Pectins as mediators of wall porosity in soybean cells. *Planta* **1988**, *175*, 389–395. [[CrossRef](#)]
55. Sowa, S.; Connor, K.F.; Towill, L.E. Temperature changes in lipid and protein structure measured by Fourier transform infrared spectrophotometry in intact pollen grains. *Plant Sci.* **1991**, *78*, 1–9. [[CrossRef](#)]
56. Oleszko, A.; Olsztyńska-Janus, S.; Walski, T.; Grzeszczuk-Kuć, K.; Bujok, J.; GaBecka, K.; Czerski, A.; Witkiewicz, W.; Komorowska, M. Application of FTIR-ATR spectroscopy to determine the extent of lipid peroxidation in plasma during haemodialysis. *Biomed. Res. Int.* **2015**, *2015*, 245607. [[CrossRef](#)]
57. Narayanan, S.; Tamura, P.J.; Roth, M.R.; Prasad, P.V.V.; Welti, R. Wheat leaf lipids during heat stress: I. High day and night temperatures result in major lipid alterations. *Plant Cell Environ.* **2016**, *39*, 787–803. [[CrossRef](#)] [[PubMed](#)]
58. Xanthopoulos, P.; Pardalos, P.M.; Trafalis, T.B. Linear discriminant analysis. In *Robust Data Mining*; Springer Briefs in Optimization; Springer: New York, NY, USA, 2012; pp. 27–33. [[CrossRef](#)]
59. Harrison, D.; Rivard, B.; Sánchez-Azofeifa, A. Classification of tree species based on longwave hyperspectral data from leaves, a case study for a tropical dry forest. *Int. J. Appl. Earth Obs. Geoinf.* **2018**, *66*, 93–105. [[CrossRef](#)]
60. Álvarez, Á.; Yáñez, J.; Neira, Y.; Castillo-Felices, R.; Hinrichsen, P. Simple distinction of grapevine (*Vitis vinifera* L.) genotypes by direct ATR-FTIR. *Food Chem.* **2020**, *328*, 127164. [[CrossRef](#)]
61. Bona, E.; Marquetti, I.; Link, J.V.; Makimori, G.Y.F.; da Costa Arca, V.; Lemes, A.L.G.; Ferreira, J.M.G.; dos Santos Scholz, M.B.; Valderrama, P.; Poppi, R.J. Support vector machines in tandem with infrared spectroscopy for geographical classification of green arabica coffee. *LWT Food Sci. Technol.* **2017**, *76*, 330–336. [[CrossRef](#)]
62. Setser, A.L.; Smith, R.W. Comparison of variable selection methods prior to linear discriminant analysis classification of synthetic phenethylamines and tryptamines. *Forensic Chem.* **2018**, *11*, 77–86. [[CrossRef](#)]
63. Stuart, B. Spectral analysis. In *Infrared Spectroscopy: Fundamentals and Applications*; Stuart, B., Ed.; John Wiley & Sons Ltd.: Chichester, UK, 2004; pp. 45–70.
64. Zampieri, M.; Ceglar, A.; Dentener, F.; Toreti, A. Wheat yield loss attributable to heat waves, drought and water excess at the global, national and subnational scales. *Environ. Res. Lett.* **2017**, *12*, 064008. [[CrossRef](#)]
65. Paymard, P.; Yaghoubi, F.; Nouri, M.; Bannayan, M. Projecting climate change impacts on rainfed wheat yield, water demand, and water use efficiency in northeast Iran. *Theor. Appl. Climatol.* **2019**, *138*, 1361–1373. [[CrossRef](#)]